Electrocatalysis (2017) 8:509–517
DOI 10.1007/s12678-017-0380-z

ORIGINAL RESEARCH

Electrocatalytic Oxidation of Formate and Formic Acid on Platinum and Gold: Study of pH Dependence with Phosphate Buffers

Areeg Abdelrahman[1] · **Johannes M. Hermann**[1] · **Ludwig A. Kibler**[1]

Published online: 5 May 2017

Abstract The effect of electrolyte pH on the electrooxidation of formic acid/formate is studied using cyclic voltammetry on polycrystalline rotating disk and single-crystalline Pt and Au electrodes in phosphate-based solutions over a wide range of pH (1–12). A non-linear relationship between oxidation current and pH at constant overpotential is identified for both metals. Surface structure influences the reaction for both Pt and Au electrodes. The results in terms of pH dependence are in agreement with those reported in literature. However, experimental evidence shows that adsorbed phosphates cause dramatic changes in the behaviour of the oxidation of formic acid on Pt and Au electrodes due to site blocking and competitive adsorption. The pH dependence on the catalytic activity for formic acid oxidation on Pt is more complex, due to the poisoning of the electrodes by adsorbed CO in addition to intricate anion adsorption effects. The role of the phosphates in the electrocatalyzed reaction is more than maintaining the pH of the system. Rather, various phosphate anions strongly adsorb on the surface, block reactive surface sites and quantitatively decrease oxidation currents. The blocking effect of the phosphate anions increases with increasing pH value. A more considerable blocking effect is established for Au. In addition, a strong pH dependence on overpotential is identified for Pt. In general, oxidation kinetics of formic acid depends strongly on pH, the nature of the adsorbed phosphate species and the electrode potential.

Keywords Formic acid oxidation · Anion adsorption · pH effect · Phosphate · Site blocking

Introduction

The formic acid molecule with its simple structure is ideal for fundamental studies in electrocatalysis of oxygenated organic C1 molecules [1]. Formally composed of molecular hydrogen and carbon dioxide, two chemical bonds have to be split during complete oxidation. As weak acid with a pK_a of 3.78 [2], it is present essentially as formate in alkaline media, and only the C–H bond has to be broken. Several recent observations show that the electrocatalytic oxidation of formic acid exhibits different kinetics in alkaline media compared to acidic media [3–9]. Some studies established that the electrooxidation of formic acid in acidic media is a lot faster than that of formate in strong alkaline media (pH = 14) [8]. Others showed that the oxidation currents of Pt increase with an increase in the molar ratio of $HCOO^-$ at pH <5 [3, 4, 7]. Therefore, probing the reaction over a wide pH range is crucial to obtain a deeper understanding of the formic acid oxidation mechanism and to improve its technological applications.

Among the most suitable buffers for such a purpose are phosphate buffers [10–12]. However, it should be taken into account that a change in the chemical nature of adsorbing species is likely with changing pH, since phosphoric acid has three dissociation constants. In turn, different adsorption strengths are expected depending on the pH of the electrolyte, electrode potential, and chemical nature and surface structure of the substrate. It is essential to note the effect of the nature of spectator anions, which could adsorb on the electrode surface more strongly than reactive molecules or reaction intermediates. Together with the solution pH, the different adsorption strengths of spectator species could critically influence the

Electronic supplementary material The online version of this article (doi:10.1007/s12678-017-0380-z) contains supplementary material, which is available to authorized users.

✉ Ludwig A. Kibler
ludwig.kibler@uni-ulm.de

[1] Institut für Elektrochemie, Universität Ulm, 89069 Ulm, Germany

reaction kinetics and eventually the reaction mechanism. It is the principal purpose of the present work to study such adsorption effects besides the pure pH effects.

Recent studies carried out with polycrystalline Pt in phosphate-based electrolytes show bell-shaped pH dependence for formic acid oxidation peaked at a pH close to the pK_a of HCOOH [10, 11]. These findings were corroborated by a theory which states that for a two-proton–electron transfer reaction, the optimal pH for catalysis is close or equal to the pK_a of the key intermediate [13]. In addition, the decrease in currents at pH > pK_a of HCOOH was explained by the formation of surface oxides and/or the adsorption of hydroxyl species (OH_{ads}) which causes increased site blocking of the surface [10, 11]. However, similar studies, also carried out on polycrystalline Pt electrodes in different electrolytes (sulphate/perchlorate), show that the electrocatalytic activity increases with increasing pH until pH ≈ 5, followed by a plateau up to pH ≈ 10 [14]. The distinct difference in pH dependence for HCOOH oxidation on polycrystalline Pt in the presence of different anions clearly indicates that the optimum catalytic activity should not necessarily occur at a pH close to the pK_a of the key intermediate and that OH_{ads} is not the reason for the decrease in oxidation currents at pH above the pK_a of HCOOH. Such inconsistencies in experimental findings indicate that this theory should be revisited. Instead, the combined effects of pH and adsorption of specifically adsorbing anions (in this case phosphate) clearly influence the mechanism for formic acid oxidation.

The electrooxidation of formic acid is classified by a dual-path mechanism [15], since the molecule is made up of H_2 + CO_2 or H_2O + CO. In the direct path, formic acid is directly transformed to carbon dioxide via a reactive intermediate. In the indirect path, which mainly occurs on Pt, a strongly adsorbed CO intermediate blocks the surface and impedes further oxidation of formic acid [16–20]. Nevertheless, the nature and role of the surface-bonded intermediate involved in this route has been liable to much debate [21, 22]. Recent experimental findings have indicated that a main adsorbate resulting from formic acid dehydrogenation on several noble metals, including Pt and Au, is formate [23–26]. Using similar experimental techniques, other findings have indicated that in acidic solutions, formate is a spectator instead [27, 28]. Theoretical studies performed on Pt have also shown disagreement on the nature of adsorbed intermediate and the role of formate on the reaction mechanism [29, 30]. Moreover, a recent study for formic acid oxidation on Au(111) shows that formate adsorbed in different configurations can play the role either of a reactive intermediate or of a strongly chemisorbed spectator species [31].

Extensive research has been devoted to polycrystalline Pt electrodes due to their specific catalytic properties for formic acid oxidation [4, 7, 10–12, 14, 16, 30, 32]. Unlike Pt though, Au is not poisoned by the adsorption of CO [15, 33]. Hence, despite of its lower activity, the use of Au electrodes may provide a simpler understanding of the reaction mechanism. In addition, since the electrooxidation of formic acid is very structure-sensitive [34], the use of well-ordered surfaces with low index planes would help provide detailed information of its reaction kinetics.

Hence, the aim of this paper is to clarify the combined effects of several experimental parameters such as solution pH, presence of strongly adsorbing anions and electrode surface structure on the electrooxidation of formic acid/formate on Pt and Au electrodes. Systematic measurements using cyclic voltammetry, in phosphate-buffered supporting electrolytes over a wide pH range (1–12), are performed on polycrystalline rotating disk and single-crystalline electrodes with (111) surface orientation. Emphasis is put on the fact that the role of the phosphates in the electrocatalyzed reaction is more than maintaining the pH of the system. The pH dependence of Pt and Au electrodes for formic acid oxidation is greatly affected by the specific adsorption of phosphate anions, which act as spectators in this model catalytic reaction. In this way, the co-adsorption of formate and phosphate ions and the effect on the electrocatalysis of Pt and Au electrodes for formic acid oxidation is studied. It will be shown that phosphate anions block reactive surface sites, which results in a dramatic decrease in electrocatalytic activity.

Experimental

A conventional three-electrode thermostatic glass cell was used to perform cyclic voltammetric experiments at 293 K. All experiments were conducted using a HEKA PG 590 or an Autolab PG128N potentiostat–galvanostat. A Pt wire and a graphite rod served as the counter electrodes for experiments with Au and Pt electrodes acting as the working electrodes, respectively. A saturated mercury sulphate electrode (MSE) connected to the cell via a Luggin–Haber capillary served as the reference electrode. Potentials in this study refer to the standard equilibrium potential for the oxidation of formic acid (η), after taking into account the activity of $HCOOH_{(aq)}$ and $CO_{2(aq)}$ and correcting of the thermodynamic effect of the pH on the electrode potentials [35]. The overpotential (η) is defined as the difference between the measured electrode potential and the standard equilibrium potential.

Pt and Au rotating disk electrodes (RDE) were used. The rotation rates were controlled by a CVT-101 Radiometer apparatus. Prior to the initial use of Pt and Au (RDE), traces of contaminations were removed by electrochemical polishing and a chemical treatment, respectively. Pt and Au single-crystalline electrodes with (111) surface orientation were also used and prepared by using a flame annealing treatment. Prior to each experiment, Pt electrodes were electrochemically cleaned (cycling between surface oxidation and hydrogen

adsorption–desorption regions) in 0.1 M H_2SO_4 until stable voltammograms were obtained. On the other hand, the quality of Au electrode surfaces was checked by their cyclic voltammetric profile (at potentials negative of the region of surface oxidation) in 0.1 M H_2SO_4.

All solutions were prepared using Milli-Q water (18.2 MΩ cm at 25 °C, TOC <2 ppb). In nearly all experiments, 0.2 M phosphate buffer solutions prepared from H_3PO_4 (Merck, Suprapur), NaH_2PO_4 or Na_2HPO_4 (Sigma-Aldrich, 99.999%) and Na_3PO_4 (Sigma-Aldrich, ≥98%) with pH values between 1 and 12 functioned as the supporting electrolyte. A few experiments required the use of other chemicals such as $HClO_4$ (Merck, Suprapur) to bring the pH down to values less than 1.5. Added to the electrolyte is 50 mM NaHCOO (Sigma-Aldrich, 99.998%) which served as the source of $HCOOH/HCOO^-$. All chemicals are used as received without further purification. Solutions were purged with nitrogen, preceding and during the experiments.

During the electrooxidation of formic acid, it is essential to insure that the electrochemical release of protons during the oxidation reaction does not significantly change the local pH at the electrode surface. This change would affect the rate of reaction and alter the relationship between the electrocatalytic activity of the electrode and the solution pH, providing misleading results. It is very difficult, however, to insure that such change does not take place during the experiment. Therefore, a 'pHenomenal' pH probe (VWR International) was used to measure the electrolyte solution before and after purging with nitrogen and after formate addition. No attempt was made to control the pH at a constant value. No significant difference was noted in the pH of the buffered supporting electrolyte solution before and after purging with nitrogen. However, unlike what is stated in [10, 11], a significant difference could be noticed once NaHCOO was added as the source of formate, especially at pH values ranging from 2 to 5.

Results and Discussion

Influence of pH on HCOOH Electrooxidation at Platinum Electrodes

Investigations of HCOOH electrooxidation using polycrystalline Pt rotating disk electrodes in phosphate-based solutions have recently been reported [10–12]. For the sake of comparison, similar measurements have been performed. Current–potential curves for Pt (RDE) at 1000 rpm in 0.2 M phosphate-buffered supporting electrolyte + 0.05 M HCOOH are recorded for pH values ranging from 1 to 12 (Fig. 1).

Although the RHE scale is often used to characterize optimum catalytic activity, the overpotential is a more straightforward representation since it also takes into account the activity of carbonic acid [35]. Representative oxidation curves as a function of overpotential at various pH values are plotted in Fig. 1. The values chosen represent the main pH values of interest, close to the pK_a of formic acid/formate and pK_{a1} and pK_{a2} of phosphate.

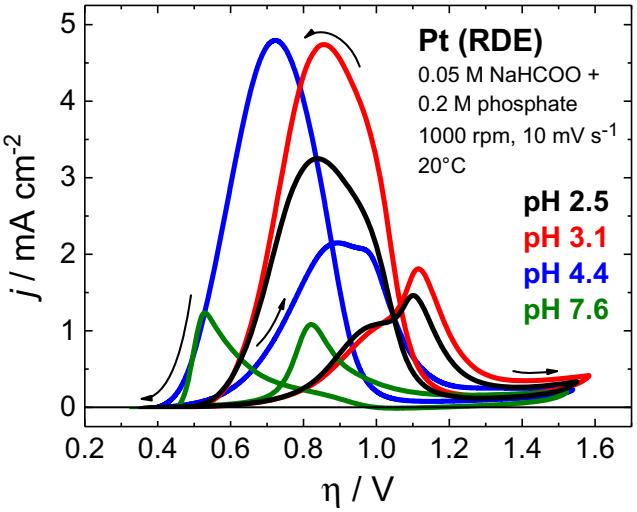

Fig. 1 Current–potential curves for the oxidation of formic acid on a Pt (RDE) in 0.05 M NaHCOO + 0.2 M phosphate-buffered solutions at different pH values. Rotation rate 1000 rpm. Scan rate 10 mV s^{-1}

Partial suppression of hydrogen adsorption shows some CO poisoning. For pH <5, as the potential increases, formate adsorption and formic acid electrooxidation are enabled as partial CO_{ads} oxidation reveals a number of active sites. Hence, the two oxidation peaks in the positive scan and the single peak in the negative scan. For pH >5, current–potential curves become simpler with only one oxidation peak in each scan direction. There is a non-linear behaviour between peak current densities at constant overpotential and pH. As the pH increases, peak current densities continue to increase gradually, reach a maximum at pH 4.4 then decrease again.

It should be noted that for all pH values, measurements with and without rotation (not shown) of the electrode have been performed. The effect of rotation and gradually increasing rotation rates from 1000 to 5000 rpm on current values and voltammetric features of the Pt (RDE) is negligible. This shows that the electrooxidation of formic acid/formate on Pt is primarily controlled by reaction kinetics and not by mass transport. The results, in terms of voltammetric profiles, pH dependence and effect of electrode rotation, are in agreement with those reported in literature [10–12]. A small variation in current densities can be attributed to several factors. Most important are (i) the use of slightly different phosphate concentrations in the supporting electrolyte, hence altering the composition of species in solution, and (ii) changes in the surface roughness of the Pt surfaces as a result of the different pre-treatment of the working electrodes.

Analogous experiments in literature were also carried out with the Pt RDE in the presence of sulphate or perchlorate, where the electrocatalytic activity increases with increasing

pH until pH ≈ 5, followed by an activity plateau up to pH ≈ 10 [12, 14]. This behaviour is distinctly different from that in phosphate-based electrolytes [10, 11]. In this case, the decrease in oxidation currents at pH >3.7 was explained by the formation of surface oxides and/or the adsorption of hydroxyl species (OH_{ads}) which would cause increased site blocking of the surface. However, for a constant pH value, OH_{ads} on its own would not explain the distinct difference in pH dependence for HCOOH oxidation on polycrystalline Pt in the presence of different anions.

According to these observations, we felt the need to understand the reason for different current–pH dependencies in the presence of various specifically adsorbing anions. Since the study of formic acid/formate oxidation and anion adsorption is strongly influenced by surface structure, measurements in the same electrolyte are performed for various pH values using a well-ordered Pt(111) single-crystal electrode. In addition, gold electrodes are more appropriate to carry out these measurements since no CO poisoning takes place on the electrode surface and due to the fact that gold electrodes are less sensitive to OH adsorption than platinum electrodes. For the sake of comparison, similar measurements are also carried out on a polycrystalline Au (RDE) and Au(111) single-crystal electrode.

Current–potential curves of Pt(111) in 0.2 M phosphate-buffered solutions + 0.05 M HCOOH are recorded for pH values ranging from 1 to 12 (Fig. 2). These measurements show that the influence of pH on the electrooxidation of formic acid for Pt electrodes is structure-sensitive in terms of the general voltammetric profiles.

For pH <2, two oxidation peaks appear in the positive scan, and after the reduction of surface oxide in the negative scan, a single peak appears (Fig. 2a). As the pH increases, the second peak in the positive scan, which is located at more positive overpotentials, disappears gradually until a single peak forms. Figure 2 shows that in general, the anodic peaks appear at almost identical potentials in both the positive and negative scans. This indicates that for this pH range, the CO coverage on the Pt(111) electrode is not as high as that on Pt (RDE).

In principle, the pH dependence for both Pt electrodes is similar. However, the highest current densities are obtained for an electrolyte pH of 4.4 and 5.1–5.4 for Pt (RDE) and Pt(111), respectively, which means that the maximum electrocatalytic activity is not solely defined by the properties of the reactive species, e.g., the pK_a of formic acid. This difference could be explained by the different adsorption strengths of phosphates and/or different potential regions where the adsorption of OH takes place on both electrodes. It should also be noted that the pH of maximum activity changes with varying scan rate in the case of Pt(111). More specifically, for a scan rate of say 50 mV s^{-1}, the peak maximum occurs at pH 4.4 already.

Figure 3 shows a plot of the onset overpotentials of oxidation for both Pt (RDE) and Pt(111) taken from the negative scans. The onset potential was arbitrarily defined as the overpotential at which the current density goes below 10 μA cm^{-2}.

The plot in Fig. 3 indicates that onset overpotentials are clearly influenced by the surface structure for pH >8. For pH values up to 8, both electrodes show an almost constant onset potential of ca. 0.47 V. Above pH 8, while the pH dependence on the onset potentials for Pt (RDE) is not prominent, an obvious increase to more positive overpotentials is identified for Pt(111). HPO_4^{2-} species are already present in the solution and could possibly be adsorbing on Pt(111) more strongly than on Pt (RDE).

Influence of pH on HCOOH Electrooxidation at Gold Electrodes

The potentiodynamic oxidation of formic acid/formate on a polycrystalline Au (RDE) at 1000 rpm in 0.2 M phosphate-buffered supporting electrolyte + 0.05 M HCOOH with pH values ranging from 1 to 12 is investigated. Similar measurements are performed for the same pH values on an Au(111) single crystal electrode. Figure 4 compares the oxidation curves of the Au (RDE) and the Au(111) electrode as a function of the overpotential. Since formic acid oxidation is greatly affected by the presence of surface oxides [33], both electrodes are cycled to potentials where structural changes of the Au surfaces are avoided. For the sake of simplicity, only the positive scans of the voltammograms performed for pH <7

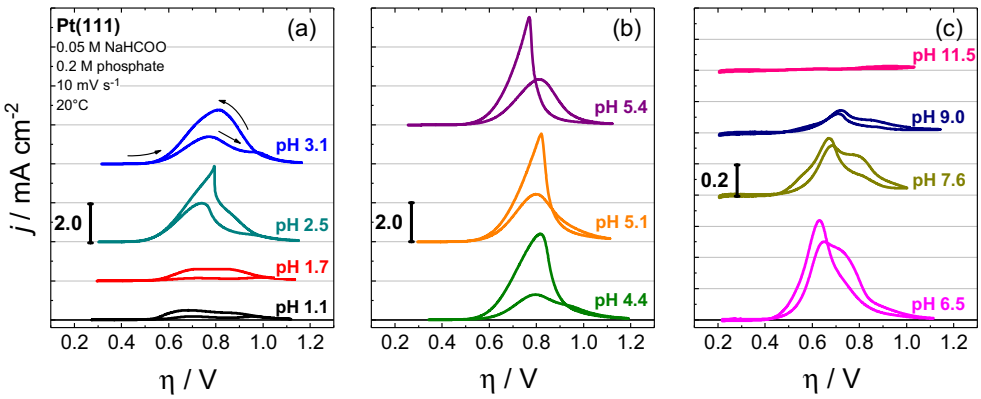

Fig. 2 Current–potential curves for the oxidation of formic acid on a Pt(111) electrode in 0.05 M NaHCOO + 0.2 M phosphate-buffered solutions at different pH values. Scan rate 10 mV s^{-1}

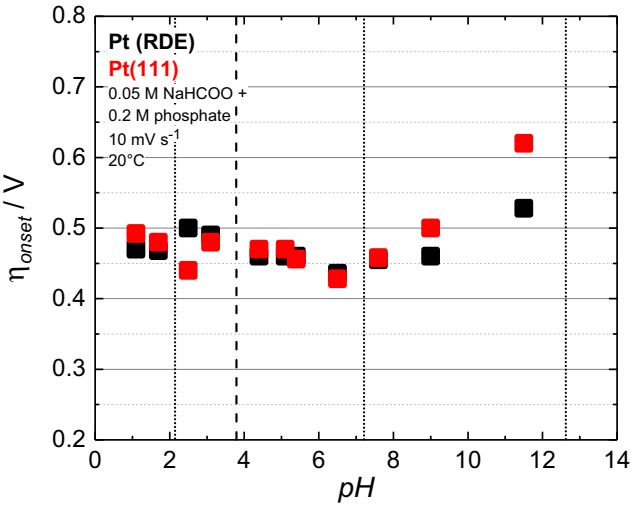

Fig. 3 Plot of onset overpotentials versus pH for formic acid oxidation (negative scan) on a Pt (RDE) and a Pt(111) electrode (*black* and *red lines*; respectively) in 0.05 M NaHCOO + 0.2 M phosphate-buffered solutions at different pH values. Rotation rate (RDE) 1000 rpm. Scan rate 10 mV s^{-1}. Dissociation constants of HCOOH, $HCOO^-$ (*broken line*) and phosphate buffer (*dotted lines*)

are displayed. At higher pH values, oxidation curves look very similar to those at pH 6.5 but with lower current densities (not shown). The electrocatalytic activity decreases steadily up to pH 11.5.

It is obvious that similar to the Pt (RDE), the Au (RDE) shows a non-linear relationship between solution catalytic

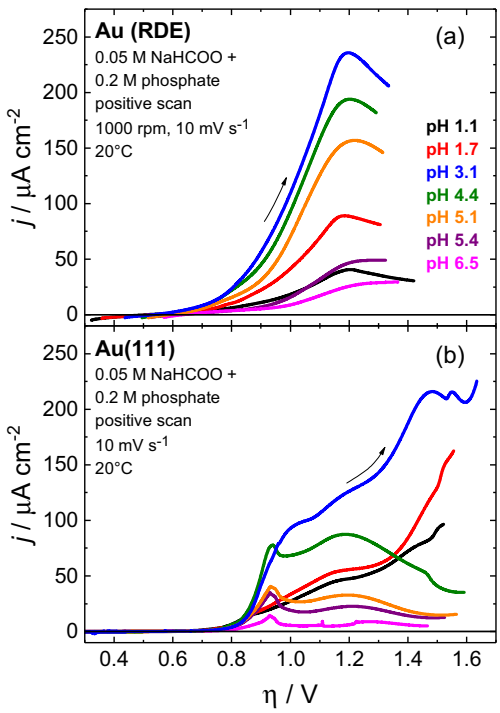

Fig. 4 Current–potential curves (positive scans) for the oxidation of formic acid on an **a** Au (RDE) and **b** Au(111) electrode in 0.05 M NaHCOO + 0.2 M phosphate-buffered solutions at different pH values. Rotation rate (RDE) 1000 rpm. Scan rate 10 mV s^{-1}

activity and pH (Fig. 4a). The Au (RDE) shows much lower catalytic activity for formic acid oxidation, compared with that of Pt. The electrocatalytic activity increases with increasing pH to achieve a maximum current density of 230 µA cm^{-2} at 1.2 V for pH 3.1, followed by a decrease again as the pH increases further. At even higher pH values, catalytic activities decrease again and reach maximum current densities much lower than those for acidic solutions.

It should be noted that no hysteresis is found for both the positive and negative scan directions of the cyclic voltammograms between 0.4 and 1.4 V (not shown), which is in agreement with the absence of CO poisoning on Au. In addition, for the Au (RDE), oxidation currents and voltammetric profiles are independent of rotation and/or rotation rates (1000–5000 rpm), verifying that formic acid/formate electrooxidation is not controlled by mass transport limitations under the present experimental conditions.

Measurements using an Au(111) electrode (Fig. 4b) show that independent of surface structure, there is an influence of pH on the electrooxidation of formic acid with a maximum current density of 125 µA cm^{-2} at 1.2 V, again for pH 3.1. The reaction is, however, strongly structure-sensitive, in terms of the general details of the current–potential curves, which are clearly different for both the polycrystalline (RDE) and the single-crystalline electrode. Unlike the polycrystalline sample, Au(111) has no specifically identifiable maximum current density peaks for the oxidation reaction at pH <4. At pH >4, the small narrow peaks at ca. 0.93 V relate to the lifting of the reconstructed Au(111) surface. In addition, a characteristic current kink can be seen at more positive potentials for pH <5. This kink is observed for well-ordered Au(111) surfaces also in the absence of the phosphate buffer and is related with a phase transition within the adsorbed formate adlayer [31]. At pH >6, HPO_4^{2-} and PO_4^{3-} form a stable structure and undergo adlayer phase transition after the lifting of reconstruction at more positive overpotentials [36, 37]. The adsorption of HPO_4^{2-} and PO_4^{3-} occurs at ca. 0.85–1.15 V versus RHE for pH ≈ 6.4 [38]. It is interesting to point out that the anodic spikes in the current–potential curves in Fig. 4b start to appear at pH 6.5 and are practically in the same potential range.

Surface structure also has a slight effect on the onset of oxidation for all pH values as seen in Fig. 5. The onset potential is chosen to be the overpotential where the formic acid oxidation current becomes lower than 1 µA cm^{-2} in the negative scan. For comparison, the same criterion is used for the Au (RDE). In acidic electrolyte (pH <5), E_{onset} for both electrodes is at constant overpotential, where formate adsorption is accompanied by simultaneous proton and electron transfer reactions. For this pH region, the onset of oxidation in the case of the Au(111) is shifted slightly to more positive overpotentials, compared to the Au (RDE). This could be explained by the more positive potential of zero charge of the Au(111) surface. For higher pH values (pH 5–9), the onset

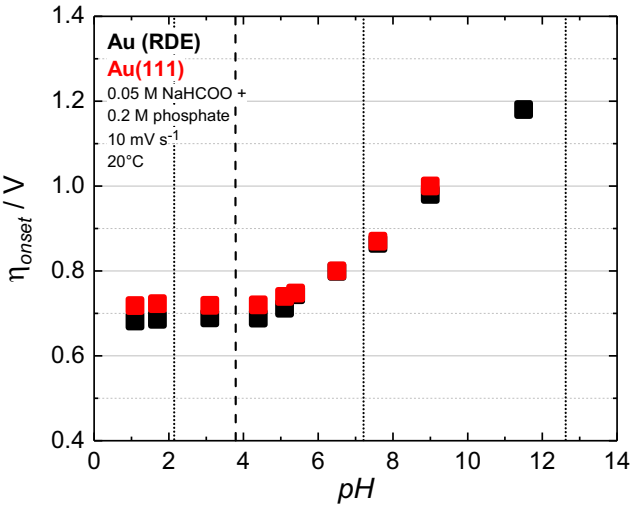

Fig. 5 Plot of onset overpotentials versus pH for formic acid oxidation (negative scan) on an Au (RDE) and an Au(111) electrode (*black* and *red lines*; respectively) in 0.05 M NaHCOO + 0.2 M phosphate-buffered solutions at different pH values. Rotation rate (RDE) 1000 rpm. Scan rate 10 mV s^{-1}. Dissociation constants of HCOOH, $HCOO^-$ (*broken line*) and phosphate buffer (*dotted lines*)

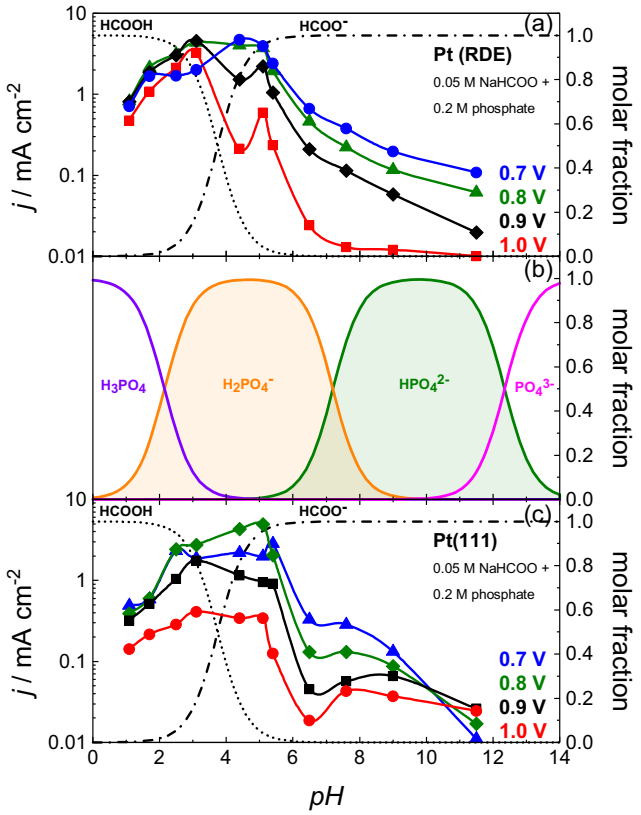

Fig. 6 Plot of oxidation current densities at constant overpotentials for the oxidation of formic acid (negative scan) versus pH on a **a** Pt (RDE) and **c** Pt(111) electrode in 0.05 M NaHCOO + 0.2 M phosphate-buffered solutions. Rotation rate 1000 rpm. Scan rate 10 mV s^{-1}. Molar fractions of HCOOH, $HCOO^-$ (*dashed traces*) and phosphate buffers (*coloured traces*) shown in **b**

of oxidation of both Au (RDE) and Au(111) is shifted by approximately 60 mV per decade to more positive overpotentials. This finding signifies that for this electrocatalytic reaction, the adsorption of formate plays an essential role.

Influence of Phosphate Anions on HCOOH Electrooxidation at Platinum

Due to the co-adsorption of CO, which increases with increasing pH, and the surface oxidation of Pt, hysteresis is seen in oxidation curves of the positive and negative scans. To avoid any significant CO poisoning, oxidation current densities in the negative scans for the Pt (RDE) and the Pt(111) electrode have been plotted versus pH at constant overpotentials (Fig. 6). The molar fractions of the different phosphate species in the supporting electrolyte are represented as the coloured traces in Fig. 6.

It is clear from the plot that the pH dependence of HCOOH oxidation on the current densities is strongly influenced by overpotential. To determine the electrocatalytic activity of formic acid oxidation on Pt (RDE) with respect to the molar fraction of formic acid and formate in solution, the plot in Fig. 6a can be divided into three regions for overpotentials greater than 0.7 V. As can be seen, there is an increase in electrocatalytic activity until pH 3. At these low pH values there is still undissociated formic acid present in solution. Nonetheless, the increase in anodic current density with increasing pH is supposed to be caused by an increase in the molar fraction of $HCOO^-_{(aq)}$.

For pH >3 up to pH ≈ 4.5, the current density continues to increase for lower overpotentials (η = 0.7 V) due to the increase of the $HCOO^-$ molar fraction. In spite of the further increase until pH 5, anodic currents decrease at higher overpotentials and this decrease becomes more pronounced with increasing overpotential. Such a change in the reaction behaviour could be related to the nature of the adsorbed species found on the electrode surface. It must be noted that the true pK_a of species at the electrode surface changes from that of the bulk solution. It is also complicated to identify particular phosphate species at the interphase in a certain pH region due to different adsorption configurations. However, FTIR studies have established clear changes in the nature of phosphate anions and related bands with pH and potential on polycrystalline Pt [39]. Adsorbed phosphate species dissociate on the surface of the electrode at more positive potentials. For 3> pH >4.5, $H_2PO_4^-{}_{(aq)}$ is the predominant species in solution. Adsorbed $H_2PO_4^-$ shows two different configurations in mildly acidic solution (pH ≈ 3) [39]. Below 0.8 V versus Pd/H_2, it is adsorbed onto the surface via two oxygen atoms [39]. Above 0.9 V versus Pd/H_2, $H_2PO_4^-$ transforms to single coordination due to the presence of PtOH [39]. This indicates that competition between $HCOO^-$ and $H_2PO_4^-$ anions takes place. At high overpotentials, free adsorption sites are blocked

by H_2PO_{4ad} and OH_{ad} which hamper further adsorption and oxidation of formate.

A slight increase again in current density at pH ≈ 5 could be explained by one of two ways. First, once $HCOO^-$ is the predominant species, the adsorption of $H_2PO_4^-$ is not strong enough at relatively high overpotentials to hinder the oxidation reaction. Second, since at this pH region $H_2PO_4^-$ is already adsorbed on the surface, the presence of OH at low coverage could catalyse the reaction [40, 41]. Either way, it is only reasonable to propose an explanation of such a trend.

A sudden decrease in the current densities is evident at 5< pH <11. This decrease is attributed to the increase in site blocking by adsorbed phosphate species. The $HCOO^-$ concentration in solution is constant from pH 5 onward, while the mole fraction of strongly adsorbing phosphate species ($H_2PO_4^-$ and PO_4^{3-}) increases. These species compete even stronger and thus block the free sites more efficiently, hence decreasing the activity further. At pH >9, co-adsorption of formate, phosphate anions and surface hydroxide decreases oxidation currents dramatically to even lower values than those of highly acidic solutions.

Figure 6c shows that the optimum catalytic activity of the Pt(111) electrode, like the Pt (RDE), changes with changing overpotential. As the $HCOO^-$ concentration increases, the activity increases up to pH ≈ 3. Between pH 3 and 5, the activity continues to increase for low overpotential (η < 0.8 V) but decreases for higher overpotentials. In mildly acidic solutions (pH ≈ 3), the adsorbed species is $H_2PO_4^-$ at low potentials and HPO_4^{2-} at higher potentials (0.7 V vs. Pd/H_2) [42]. The presence of more strongly adsorbing HPO_4^{2-} could explain the decrease in activity in this pH region. It is possible that at higher pH values $H_2PO_4^-$ and HPO_4^{2-} adsorb on the surface and dissociate to HPO_4^{2-} and PO_4^{3-} at higher potentials. Again, the adsorption of phosphates slows down the HCOOH oxidation reaction and changes from a competition with formate at low pH values to a competition with adsorbed OH at high pH values. This competition influences the blocking effect of phosphate anions, which becomes relatively larger with increasing pH. Interestingly, the strongest phosphate blocking effects take place on Pt(111) when the pH is close to the dissociation constants of the phosphate species.

Influence of Phosphate Anions on HCOOH Electrooxidation at Gold

Figure 7 shows the current densities of the positive scans for the Au electrodes at constant overpotentials between 1.0 and 1.3 V. Four pH regions can be distinguished for Au (RDE) in Fig. 7a. At pH <3, a steady increase in oxidation currents with increasing pH is attributed to the increase in concentration of $HCOO^-_{(aq)}$. The adsorption and oxidation of $HCOO^-$ is however blocked by the adsorption of phosphates. This is why for all overpotentials, the maximum oxidation current densities

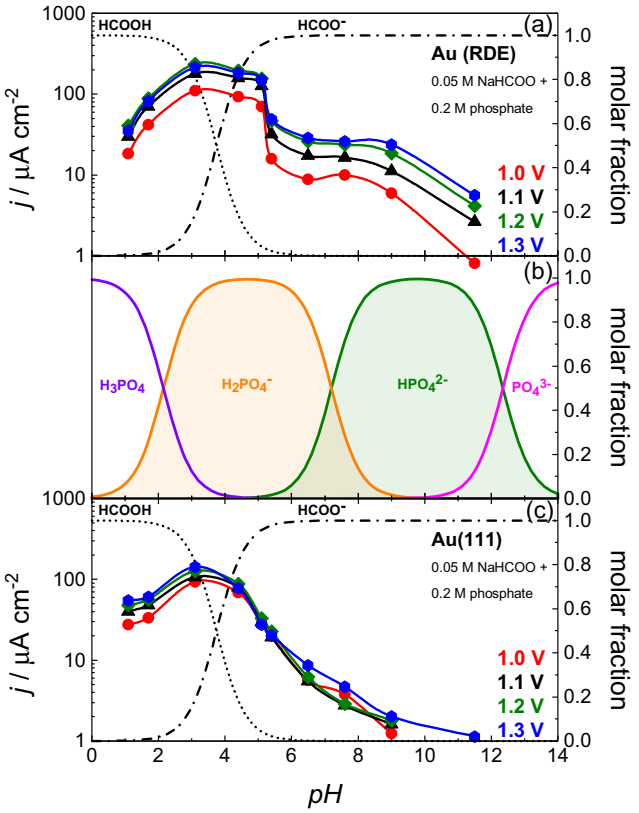

Fig. 7 Plot of oxidation current densities at constant overpotentials for the oxidation of formic acid (positive scan) versus pH on an **a** Au (RDE) and **c** Au(111) electrode in 0.05 M NaHCOO + 0.2 M phosphate-buffered solutions. Rotation rate 1000 rpm. Scan rate 10 mV s^{-1}. Molar fractions of HCOOH, $HCOO^-$ (*dashed traces*) and phosphate buffers (*coloured traces*) shown in **b**

are at pH ≈ 3, close to the first dissociation constant of phosphoric acid (pK_{a1} = 2.12) and HCOOH (pK_a = 3.75).

For 3< pH <5, the competition of anions for free active sites causes a decrease in currents. FTIR studies on the phosphate adsorption on Au [38, 43] have shown that unlike the case of Pt, in mildly acidic solutions (pH ≈ 4) only bands related to the adsorption of $H_2PO_4^-$ are present. The competition between $HCOO^-$ and $H_2PO_4^-$ decreases the current slightly but $H_2PO_4^-$ anions in this pH range do not act as site-blocking species. At pH >5, currents dramatically decrease. A possible explanation for this behaviour is that for pH ≈ 6, the onset of adsorption of HPO_4^{2-} and PO_4^{3-} occurs at almost the same potential (0.6 V Pd/H_2) [38, 43]. HPO_4^- is probably triply coordinated and adsorbs to the Au(111) surface via three oxygen atoms [38]. The strong chemisorption of HPO_4^{2-} (and PO_4^{3-}) leads to substantial site blocking and almost complete deactivation of formate oxidation.

Figure 7c shows a similar plot for the oxidation current densities of the Au(111) electrode at the same overpotentials plotted versus pH. This plot can be divided into three regions. Like the case of polycrystalline Au, the current density

increases until pH 3 for each overpotential. This is again attributed to the increase in $HCOO^-$ concentration. In contrast to polycrystalline Au, there is only a small change in catalytic activity between pH values 1.1 and 1.7 for Au(111). This is probably due to the fact that the latter pH lies close to pK_{a1} (2.16) of phosphate and this causes a more strongly bound phosphate to adsorb on the well-ordered Au(111) electrode. The maximum oxidation current density is found at pH ≈ 3 for all constant overpotentials.

For 4> pH >11, oxidation current densities decrease steadily with increasing pH and are almost identical at all overpotentials. This finding signifies that for this pH region, around pK_{a1} and pK_{a2} (2.16 and 7.21) of phosphate, the catalytic activity is limited by the number of free adsorption sites. At higher overpotentials, the driving force which causes currents to increase is compensated by the blocking of active surface sites. While the coverage of phosphate species increases with potential, the number of free sites available for formate oxidation decreases. The blocking of active sites caused by phosphate is so strong, even at high overpotentials that, in contrast to polycrystalline Au, Au(111) does not show a shoulder in catalytic activity at pH ≈ 8. At pH = 11.5, the catalytic activity for HCOOH oxidation is almost zero.

It should be noted that at pH >1.5, with the exception of pH 5.1, Au (RDE) shows a twofold to threefold increase in current densities as compared to Au(111). In the absence of phosphates, Au(111) is more active than polycrystalline Au [14]. Obviously, the adsorption of phosphates is stronger on Au(111), which leads to blocking of active sites at peak potentials. In addition, assuming that phosphate adsorption is strong on both Pt and Au surfaces, the lack of hysteresis in the pH-current density plots of Au shows that blocking of phosphate species is stronger for the Au electrodes than for the Pt electrodes.

Finally, it is worth stating that there is no simple way to define pH dependence for HCOOH oxidation for all pH values. However, in general, the dependence can be divided into two broad pH regions. Up to pH 5, the reaction depends greatly on formate ion concentration which increases with solution pH. Representing the electrocatalytic activity as a function of overpotential provides good understanding of the pH dependence of this reaction. On the other hand, for higher pH values, the catalytic activity shifts to more positive overpotentials. Therefore, determining the current densities at constant electrode potentials (not overpotentials) would be more appropriate.

The Blocking Effect of Phosphate Anions on HCOOH Electrooxidation

Preliminary measurements in our laboratory for formic acid oxidation on a Pt(111) and an Au(111) electrode in the absence of phosphate anions have been performed (not shown). For the case of Pt(111), the current densities steadily increase with increasing pH up to a pH ≈ 4 then remain almost constant till pH ≈ 8 then decrease again. For Au(111), the current densities continue to increase till pH ≈ 5 then remain constant for higher pH values. A sudden decrease in catalytic current is observed for pH >12. Therefore, we conclude that the decrease in electrocatalytic activity on both Pt and Au electrodes is strongly influenced by site-blocking phosphate-adsorbed species. This means that the buffering effect of phosphates is accompanied by substantial lowering of catalytic activity. At constant potentials, with and without the presence of phosphate anions, the decrease in currents is dramatic for the Au(111) electrode and is evident in the five times decrease in current densities at pH ≈ 5 compared to the Au (RDE) where a further increase in $HCOO^-$ concentration is not enough to drive the reaction to higher catalytic currents.

In fact, a 'blocking factor' as shown in Fig. 8 can define the extent of decrease in current density for formic acid/formate oxidation on Pt(111) and Au(111) due to phosphate adsorption. The blocking factor is calculated as the ratio of oxidation current densities at a constant potential at each corresponding pH without and with the presence of phosphate anions in solution. It is clear from the figure that the blocking effect on Au(111) is much greater than on Pt(111). This could be explained by a stronger chemisorption of phosphates for Au(111) which leads to substantial site blocking and almost complete deactivation of formate oxidation.

Conclusions

A voltammetric study of pH dependence for the oxidation of formic acid/formate on polycrystalline and single-crystalline Pt and Au electrodes in phosphate-containing solutions in a

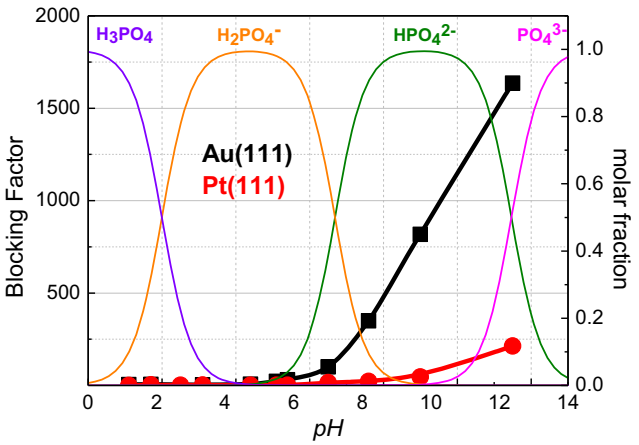

Fig. 8 Plot of the blocking factor for Pt(111) and Au(111) (calculated as the ratio of currents at a constant potential for HCOOH oxidation without and with phosphate anions in solution) versus pH. Molar fractions of phosphate buffers (*coloured traces*)

wide range of pH (1–12) has been performed. Most importantly, the effect of strongly adsorbing phosphate anions on the oxidation currents for this model electrocatalytic reaction for Pt and Au is investigated.

There is a non-linear relationship between formic acid oxidation currents and pH, independent of surface structure. This pH dependence is more complicated for the case of Pt, which is, unlike Au, easily poisoned by adsorbed CO. The dramatic decrease in catalytic activity for pH >3 in the presence of strongly adsorbing species indicates that the nature of the electrolyte anion greatly influences the oxidation of formic acid. Competitive adsorption between reactive intermediates for this reaction and strongly adsorbing anions causes pronounced changes in pH dependencies. Experimental evidence shows that phosphate anions act as site blocking spectator species and hinder further adsorption of formate. The degree of site blocking by phosphates increases with increasing pH.

Due to the different adsorption strengths of reactive and spectator species involved in the reaction, different reaction mechanisms probably take place for Pt and Au electrodes. The combined effects of pH and specific adsorption of anions other than the reactive intermediates in solution should be taken into consideration when discussing possible mechanisms for formic acid oxidation on noble metal electrodes.

Acknowledgements Financial support by the Deutsche Forschungsgemeinschaft (DFG Research Unit For-1376, Ki 787/6-1 and 6-2) and by the Fonds der Chemischen Industrie (FCI) is gratefully acknowledged.

References

1. F. Salzer, Zeitschrift Für Elektrotechnik Und Elektrochemie **8**, 893 (1902)
2. E.A. Braude, F.C. Nachod, J.G. Hoffman, Phys. Today **9**, 22 (1956)
3. R.P. Buck, L.R. Griffith, J. Electrochem. Soc. **109**, 1005 (1962)
4. R.R. Adzic, M.I. Hofman, D.M. Draizic, J. Electroanal. Chem. **110**, 361 (1980)
5. S. Chert, B. Wu, and C. Cha, **431**, 243 (1997).
6. J. Xiang, B.-L. Wu, S.-L. Chen, J. Electroanal. Chem. **517**, 95 (2001)
7. J.L. Haan, R.I. Masel, Electrochim. Acta **54**, 4073 (2009)
8. H.D. John, J. Wang, H. Rus, E.D. Abruna, J. Phys. Chem. **116**, 5810 (2012)
9. J. Jiang, J. Scott, A. Wieckowski, Electrochim. Acta **104**, 124 (2013)
10. J. Joo, T. Uchida, A. Cuesta, M.T.M. Koper, M. Osawa, J. Am. Chem. Soc. **135**, 4 (2013)
11. J. Joo, T. Uchida, A. Cuesta, M.T.M. Koper, M. Osawa, Electrochim. Acta **129**, 127 (2014)
12. J.V. Perales-Rondón, S. Brimaud, J. Solla-Gullón, E. Herrero, R. Jürgen Behm, J.M. Feliu, Electrochim. Acta **180**, 479 (2015)
13. M.T.M. Koper, Chem. Sci. **4**, 2710 (2013)
14. S. Brimaud, J. Solla-Gullón, I. Weber, J.M. Feliu, R.J. Behm, ChemElectroChem **1**, 1075 (2014)
15. A. Capon, R. Parson, J. Electroanal. Chem. Interfacial Electrochem. **44**, 1 (1973)
16. B. Beden, A. Bewick, C. Lamy, J. Electroanal. Chem. **150**, 505 (1983)
17. B. Beden, C. Lamy, N.R. de Tacconi, A.J. Arvia, Electrochim. Acta **35**, 691 (1990)
18. G. Samjeské, M. Osawa, Angew, Chemie - Int. Ed. **44**, 5694 (2005)
19. Y.X. Chen, S. Ye, M. Heinen, Z. Jusys, M. Osawa, R.J. Behm, J. Phys. Chem. B **110**, 9534 (2006)
20. Y.-X. Chen, M. Heinen, Z. Jusys, R.J. Behm, ChemPhysChem **8**, 380 (2007)
21. T.D. Jarvi, E.M. Stuve, *Electrocatalysis* (Wiley, New York, 1998), pp. 75–133
22. T. Iwasita, E. Pastor, *Interfacial Electrochem. Theory, Princ. Appl* (Marcel Dekker, Inc., New York, Basel, 1999), pp. 353–373
23. M.R. Columbia, P.A. Thiel, J. Electroanal. Chem. **369**, 1 (1994)
24. G. Crépy, C. Lamy, S. Maximovitch, J. Electroanal. Chem. **54**, 161 (1974)
25. G. Samjeské, A. Miki, S. Ye, M. Osawa, J. Phys. Chem. B **110**, 16559 (2006)
26. A. Miki, S. Ye, M. Osawa, Chem. Commun. **14**, 1500 (2002)
27. Y.X. Chen, M. Heinen, Z. Jusys, R.J. Behm, Angew, Chemie - Int. Ed. **45**, 981 (2006)
28. Y. Chen, M. Heinen, Z. Jusys, R.J. Behm, Langmuir **22**, 10399 (2006)
29. M. Neurock, M. Janik, A. Wieckowski, Faraday Discuss. **140**, 363 (2009)
30. W. Gao, J.A. Keith, J. Anton, T. Jacob, J. Am. Chem. Soc. **132**, 18377 (2010)
31. L.A. Kibler, M. Al-Shakran, J. Phys. Chem. C **120**, 16238 (2016)
32. V. Grozovski, F.J. Vidal-Iglesias, E. Herrero, J.M. Feliu, ChemPhysChem **12**, 1641 (2011)
33. A. Capon, R. Parsons, J. Electroanal. Chem. Interfacial Electrochem. **44**, 239 (1973)
34. H. H. Brongersma and R. A. van Santen, editors, *Fundamental Aspects of Heterogeneous Catalysis Studied by Particle Beams* (Springer US, Boston, MA, 1991).
35. T. Reda, C.M. Plugge, N.J. Abram, J. Hirst, Proc. Natl. Acad. Sci. **105**, 10654 (2008)
36. T. Iwasita, F. Nart, H. Gerischer, *Advances in Electrochemical Science and Engineering* (Wiley, Weinheim, 1995)
37. F. Silva, M.J. Sottomayor, A. Martins, J. Electroanal. Chem. **375**, 395 (1994)
38. M. Weber, F.C. Nart, Electrochim. Acta **41**, 653 (1996)
39. F.C. Nart, T. Iwasita, Electrochim. Acta **37**, 385 (1992)
40. L.M.C. Pinto, P. Quaino, M.D. Arce, E. Santos, W. Schmickler, ChemPhysChem **15**, 2003 (2014)
41. V. Climent, R. Gómez, J.M. Orts, J.M. Feliu, J. Phys. Chem. B **110**, 11344 (2006)
42. M. Weber, F.C. Nart, I.R. de Moraes, T. Iwasita, J. Phys. Chem. **100**, 19933 (1996)
43. M. Weber, I.R. de Moraes, A.J. Motheo, F.C. Nart, Colloids Surfaces A Physicochem. Eng. Asp. **134**, 103 (1998)